Intracellular diffusion, binding, and compartmentalization of the fluorescent calcium indicators indo-1 and fura-2

L. A. Blatter and W. G. Wier
Department of Physiology, University of Maryland, School of Medicine, Baltimore, Maryland 21201 USA

ABSTRACT We studied intracellular binding and possible compartmentalization of the fluorescent Ca^{2+} indicators, indo-1 and fura-2, in single mammalian cardiac ventricular cells that had been loaded with indo-1 and fura-2 by exposure to the acetoxymethylester form of the indicators (indo-1/AM and fura-2/AM). Techniques similar to those used in experiments on fluorescence recovery after photobleaching (FRAP) were used. It was assumed that reversible binding in myoplasm would be evident as slowed recovery of fluorescence after photobleaching, and that irreversible binding of the indicators to immobile myoplasmic sites (or "compartmentalization" in organelles) would be evident as incomplete recovery. Through the use of a mask, one half of a cell was exposed to high-intensity ultraviolet (UV) light to bleach the indo-1 or fura-2 in only that part of the cell. Upon removal of the mask and termination of the high-intensity UV illumination, fluorescence recovered in the bleached half of the cell, indicating diffusion of indo-1 and fura-2. Mathematical modeling of the diffusional redistribution of the indicators indicated that in these cells the apparent diffusion coefficent for indo-1 is 1.57×10^{-7} cm^2s^{-1} (SD 0.48×10^{-7} cm^2s^{-1}; $n = 5$ cells, 21°C), and for fura-2 is 3.19×10^{-7} cm^2s^{-1} (SD 1.85×10^{-7} cm^2s^{-1}; $n = 6$ cells, 21°C). These values are ~6 and 3, respectively, times smaller than those expected for free diffusion in the myoplasm. On the assumption that indo-1 and fura-2 bind instantaneously and reversibly to nonsaturable sites in the myoplasm, this indicates that only ~15%–20% of the diffusible indo-1 and 30–35% of the diffusible fura-2 is free in the myoplasm. In the bleached half of the cell the recovered level of fluorescence never reached the final level in the half not exposed to UV light. The extent of incomplete recovery was variable amongst the cells. Our analysis indicated that, under the conditions we used, approximately one-third of the intracellular dye is not diffusible in the myoplasm.

INTRODUCTION

The tetracarboxylate fluorescent calcium indicators, fura-2 and indo-1 (Grynkiewicz et al., 1985), have been used widely to estimate intracellular cytoplasmic free calcium ($[Ca]_i$) in various cell types. This estimation is most straightforward if the Ca^{2+} indicator is present exclusively in the cytoplasm and if its properties in the cytoplasm are the same as they are in calibrating solutions (because calibration in the cell is often impossible). The calibration curve (steady-state relationship between fura-2 fluorescence and $[Ca^{2+}]_i$) of fura-2 in toad gastric smooth muscle cells was similar, but not identical, to the calibration curve obtained in calibrating solutions (Williams et al., 1985). In cardiac muscle, an intracellular calibration of indo-1 (Spurgeon et al., 1990) was the same as a calibration curve in solutions only if it was assumed that 51% of the indo-1 was compartmentalized in mitochondria, and that the free $[Ca^{2+}]$ in the mitochondria was low. It is known that in skeletal muscle, Ca^{2+} indicators such as fura-2, arsenazo III, antipyrylazo III, dichlorophosphonazo III, azo-1, tetramethylmurexide, and purpurate indicators are bound to myoplasmic proteins and that this alters the kinetic and spectral properties of the indicators (Baylor and Hollingworth, 1988; Baylor et al., 1982, 1986; Maylie et al., 1987*a–c*; Hirota et al., 1989). Konishi and his colleagues (1988) demonstrated that in both skeletal muscle fibers and in solutions mimicking myoplasm, the binding of fura-2 to proteins influenced several properties of the indicator, such as fluorescence intensity, the fluorescence emission spectrum, the absorbance spectrum, and the dissociation constant for complexation with Ca^{2+}. Estimates of the "on" and "off" rate constants for the complexation of Ca^{2+} by fura-2 in the myoplasm are, respectively, 4 and 6–60 (Baylor and Hollingworth, 1988) times smaller than those measured in solutions (Kao and Tsien, 1988). The uncertainty in these rate constants leads to uncertainty in the estimation of $[Ca^{2+}]_i$ during rapid $[Ca^{2+}]_i$ transients (Klein et al., 1988).

Although Ca^{2+} indicators are being used extensively in mammalian cardiac muscle, these issues had not yet been investigated. Up until now, the short length of cardiac cells precluded measurements of the diffusion of Ca^{2+} indicators, that can reveal intracellular binding. Through

Address correspondence to Dr. W. G. Wier, Dept. of Physiology, School of Medicine, University of Maryland at Baltimore, 660 West Redwood St., Baltimore, MD 21201.

0006-3495/90/12/1491/09 $2.00

the use of a real-time video disk recorder and fluorescence photobleaching experiments, we now present evidence for substantial intracellular binding of both calcium indicators, indo-1 and fura-2.

Cardiac cells are often loaded with fluorescent Ca^{2+} indicator or Ca^{2+} chelator by exposure to the membrane-permeant form (acetoxymethylester [/AM]) of the indicator or chelator. This technique allows the possible entry and subsequent "trapping" of indicator in noncytoplasmic compartments such as mitochondria or other internal compartments (see e.g., Almers and Neher, 1985). The estimation of $[Ca^{2+}]_i$ from the indicator signal is problematic in such a case. We found that in cells loaded with indo-1 and fura-2 by exposure to their /AM derivatives a fraction of the indicator was not diffusible. The most likely explanation for this is the "trapping" or compartmentalization of indo-1 and fura-2 in mitochondria (see e.g., Spurgeon et al., 1990)

METHODS

Experimental set-up

The experiments were carried out in a flow-controlled perspex chamber mounted on the stage of a Nikon Diaphot microscope equipped with UV-optics (Nikon Inc., Instrument Div., Garden City, NY). The system for imaging fluorescence signals obtained from cardiac myocytes has been described in detail elsewhere (Takamatsu and Wier, 1990*a* and *b*), therefore, only a brief description will be given here. For the indo-1 measurements UV light emitted from a 75 W xenon arc lamp was made to pass through a 350 nm interference filter (30–nm bandwidth) and into an oil-immersion fluorescence objective (Nikon UV-fluor; 40× magnification; numerical aperture 1.3) for excitation of the intracellular indo-1. Fluorescence emitted from the cell passed through an interference filter (450 nm; 9-nm bandwidth) located in the side port of the microscope. For the fura-2 experiments the intracellular indicator was excited at a wavelength of 360 nm (10-nm bandwidth) and emission was recorded at 510 nm (180–nm bandwidth interference filter). The fluorescence at the side port was recorded with an intensified charge coupled device (CCD) camera (Photolux, Photonic Science, Tunbridge Wells, U. K.), which consisted of a microchannel plate intensifier (XX 1381 Philips Electronic Instruments Inc., Mahwah, NJ) coupled optically with a coherent tapered fiberoptic bundle to the CCD camera. The images obtained from the cell were processed with a real-time image processor (series 151; Imaging Technology Inc., Woburn, MA) that was controlled by a microcomputer (model 80286; Intel Corp., Santa Clara, CA). Images obtained at video frame rate (30 images per second) were stored during the experiment on a real-time video disk storage system (model 8300 RTD; Applied Memory Technology, Tustin, CA) that, thus, served as a digital framestore. Stored images were transferred to another hard disk for processing after the experiment. Computer programs for the system were written using the programming language C and the library of subroutines available from the series 151, ITEX 151 (Imaging Technology Inc.)

Cell isolation and loading with indo-1 and fura-2

The method of the enzymatic cell isolation used in our laboratory has been described in details before (Barcenas-Ruiz and Wier, 1987; Beuckelmann and Wier, 1988). Briefly, isolated hearts from adult guinea pig were subjected to retrograde arterial perfusion using the following protocol: 8 min with nominally Ca-free modified Tyrode solution (composition see below), 12 min with the modified Tyrode solution containing collagenase type I (17–18 mg/30 ml; lot No. 128F-0295; Sigma Chemical Co., St. Louis, MO) and protease type XIV (2 mg/30 ml; lot No. 87F-0106; Sigma Chemical Co.) followed by a 6-min perfusion with Tyrode solution containing 200 μmol/liter Ca. The cells were disaggregated in this solution by gentle mechanical agitation, and after filtering through a nylon mesh harvested by a three-step centrifugation procedure. The cells were stored in Tyrode solution containing 200 μmol/liter Ca.

The cells were loaded with indo-1 and fura-2 by exposure to the membrane-permeant forms, indo-1-acetoxymethyl ester and fura-2-acetoxymethyl ester, respectively (indo-1/AM lot No. 7L; fura-2/AM, lot No. 8B; Molecular Probes, Inc., Junction City, OR). A mixture of 10 μl of 1 mmol/liter indo-1/AM or fura-2/AM in dimethylsulfoxide (DMSO), 2.5 μl of 25% wt/wt Pluronic F-127 in DMSO, and 75 μl fetal calf serum (FCS) or newborn calf serum (NCS) was added to 2 ml Tyrode solution containing the cells and 40 μl FCS or NCS. Loading was achieved by gently shaking the cells for 15–30 min. A sample of the cells was then transported to the experimental chamber on the microscope stage and washed at room temperature by superfusion with Tyrode solution containing Ca^{2+} at a concentration of 200 μmol/liter. The concentration of fluorescent indicator in these cells was estimated by comparing the fura-2 fluorescence (at the excitation wavelength of 365 nm) with the fluorescence of cells perfused internally with the "free acid" form of the indicator via a micropipette electrode. The solution in the micropipette electrode contained, in addition to the usual constituents for cardiac cells (Beuckelmann and Wier, 1988), fura-2 at a concentration of 100 μM. In cells ($n = 6$) loaded with fura-2 by exposure to fura-2/AM, the average fluorescence intensity was 90% of that in cells ($n = 4$) loaded with fura-2 (free acid) via the micropipette electrode. Because the upper limit on the concentration of free fura-2 in the pipette-loaded cells was 100 μM, we conclude that the concentration of free fura-2 in the /AM loaded cells was, on average <90 μM.

The half-time of loading of fura-2 into cells via diffusion from micropipette electrodes was typically ~600 s. This is several times larger than the half-time of dye redistribution after photobleaching (see below). Nevertheless, we preferred not to study diffusion and possible compartmentalization of the free acid form of the indicator because the experiments would have been complicated greatly by having to consider the fact that the micropipette electrode constituted an additional (probably highly variable) source of unbleached indicator.

Solutions

The cells were stored and superfused during the experiments with a modified Tyrode solution of the following composition (in millimoles per liter): NaCl, 135; KCl, 4; $MgCl_2$, 1; $CaCl_2$, 0.2; dextrose, 10; Hepes, 10; NaH_2PO_4, 0.33, titrated to pH 7.3 with NaOH (~3.9 mmol/liter). For the nominally Ca-free Tyrode solution the addition of $CaCl_2$ was omitted.

Experimental protocol and data acquisition

The method chosen to investigate intracellular diffusion and binding of indo-1 and fura-2 consisted first of photobleaching one half of a dye loaded cell and then imaging the redistribution of the dye, after bleaching, using a fluorescence microscopy video imaging system. Through mathematical modeling of the redistribution of the dye as diffusion in two dimensions, an apparent intracellular diffusion coeffi-

cient (D_{app}), and the fraction of the total amount of dye that was nondiffusible, could be determined. Indo-1 fluorescence from the cell was recorded at a wavelength (450 nm) close to the isosbestic emission wavelength (455 nm) of indo-1, thus, avoiding possible changes in fluorescence signal that might arise as a result of changes in intracellular [Ca^{2+}]. For the fura-2 experiments the same was achieved by exciting the intracellular dye at the isosbestic wavelength for fura-2 (360 nm). At the beginning of an experiment, an initial fluorescence image was recorded from the unbleached cell (see Fig. 1 *B a*). For this image, the gain of the image intensifier was adjusted such that, at all pixels, the camera output was related linearly to fluorescence intensity. Indo-1 or fura-2 in one-half of the cell was then bleached by exposure for 1 min to high-intensity UV light (unfiltered emission from the xenon arc lamp, i.e., all light at wavelengths <405 nm). The indicator in the other half of the cell was protected from bleaching by an opaque mask located in the collimated UV light between xenon arc lamp and objective. Immediately after removal of the mask and at various intervals afterward fluorescence images were recorded, but with low-intensity UV light for excitation of the indo-1 (350 nm; 30–nm passband interference filter) and fura-2 (360 nm; 10-nm passband interference filter). During the intervals between the measurements the cell was not exposed to UV light in order to prevent further photobleaching of the dye. All images consist of averages of 16 successive video frames. All experiments were carried out at room temperature (21°C).

Data: fluorescence line profiles

The data consisted of linear profiles of indo-1 and fura-2 fluorescence along the longitudinal axis of the cell (see Figure 1 *A*, 1 *D*, and 2 *B*). The fluorescence profiles were obtained from spatially-filtered, background-subtracted, shading-corrected images. Background subtraction was achieved by subtracting a constant pixel value from the cell image. This value was derived from the average of 256 frames of an area of the bath which contained no cells and which was recorded at the same gain settings as the cell images. Noise reduction was achieved by spatial filtering (averaging of areas of 2 × 2 pixels). This had the result that the original 512 × 480 pixel sized image was reduced to the final size of 256 × 240 pixels. Shading correction was viewed as particularly important because this correction removed variations in fluorescence intensity that were due to inhomogeneous illumination, spatial variation in the sensitivity of the image intensifier and any other inhomogeneities introduced by the optical components. Shading correction was carried out by normalizing the cell image to an image of an indo-1 or fura-2 containing solution (for details see Takamatsu and Wier, 1990*b*): a small drop of a solution of 100 μmol/liter indo-1 salt or 50 μmol/liter fura-2 salt in 135 mmol/liter KCl was placed between two cover slips, and 256 successive frames were averaged to produce a low noise shading correcting image.

Mathematical analysis of data

The geometry of the cells, certain experimental limitations, and the possibility of reversible and irreversible binding of the intracellular indicators necessitated our approach to the analysis of the data, as described below.

Ideally, our procedure for photobleaching would have produced a step change in fluorescence in the cell in the region corresponding to the edge of the mask. This was not achieved, probably because of some redistribution of the indicators during the period of photobleaching. Because the boundary of fluorescence could not be described mathematically by a simple function, we had to use numerical methods to solve the differential equations describing diffusion in this case rather than solve analytically the equation for one-dimensional diffusion. Furthermore, several cells seemed to have significant variation in their thickness, so it was necessary to consider diffusion in two dimensions (x and z, in Fig. 1 *C*). Because the images were shading and background corrected, we assumed that variations in fluorescence intensity were due to variations in cell thickness. Fluorescence profiles along the y-axis, at different values of x, revealed relatively little variation in the central region of the cell, and, thus, diffusion in this dimension (y-axis) was ignored.

Potential binding of diffusible indo-1 and fura-2 was considered to be instantaneous in comparison to diffusion. In the absence of specific information about the affinity of potential binding sites for indo-1 and fura-2, we assumed that binding was a reversible, nonsaturable, process. At any location in the myoplasm, and at any time, the ratio (R) of bound indicator to free indicator is then constant and can be defined as:

$$R = (\text{indicator:binding site})/(\text{indicator}). \quad (1)$$

In this case, an apparent diffusion coefficient, D_{app} may be defined as:

$$D_{app} = D/(1 + R), \quad (2)$$

where D symbolizes the diffusion coefficient in the absence of reversible binding. According to Crank (1975), Eq. 2 applies whether diffusion is in one, two, or three dimensions, and irrespective of the geometry of the volume in which diffusion-with-binding is occurring. Our procedure was to determine D_{app}, as described below, and then, from published values of D for a molecule the size of indo-1 or fura-2, determine the value of R.

The irreversible binding of the dye (equivalent to compartmentalization) could be accounted if it was assumed that the fraction of the dye that was nondiffusible was constant throughout the experiment. The estimate of this fraction was independent of the estimate of D_{app}, because the simulation was run to the steady state of dye redistribution.

Numerical analysis

A line profile of fluorescence was divided into a finite number of equal-area elements in the x- and z-dimension. In each such element, C symbolizes the total amount of dye, C' symbolizes the amount of diffusible dye (which can engage in reversible binding), and C'' symbolizes the amount of nondiffusible, or irreversibly bound dye. Diffusion in each such element was allowed with one to four neighboring elements, depending on the location of the particular element within the cell. According to the finite-difference form of the diffusion equation (Crank, 1975), movement of diffusible dye in, for example, an element with four neighbors could then be described as:

$$dC'_{x,z}/dt = k_{diff} \cdot \{C'_{x+1,z} + C'_{x-1,z} + C'_{x,z+1} + C'_{x,z-1} - 4 \cdot C'_{x,z}\}, \quad (3)$$

where $C'_{x,z}$ is the amount of diffusible dye in the xth, zth element. k_{diff} is the rate constant for the movement of dye between neighboring elements, as given by Eq. 4, where x (cm) is the length of the element. (Equations similar to Eq. 3, but containing fewer terms as appropriate, were used when the number of neighboring elements was <4).

$$D_{app} = k_{diff} \cdot x^2 \quad (4)$$

Eq. 3 was solved numerically, using the program, FACSIMILE (AEA Technology, Oxfordshire, UK). The solution consisted of the amount of diffusible dye, C' as a function of time, in each element. In addition, each element was assumed to contain a constant amount of nondiffusible dye, C'', the amount of which was determined by methods described below. To produce a final model fluorescence profile analagous to what we could actually measure, C' and C'' of all elements in a column (same x, differing z's) were added together to give a predicted total amount of

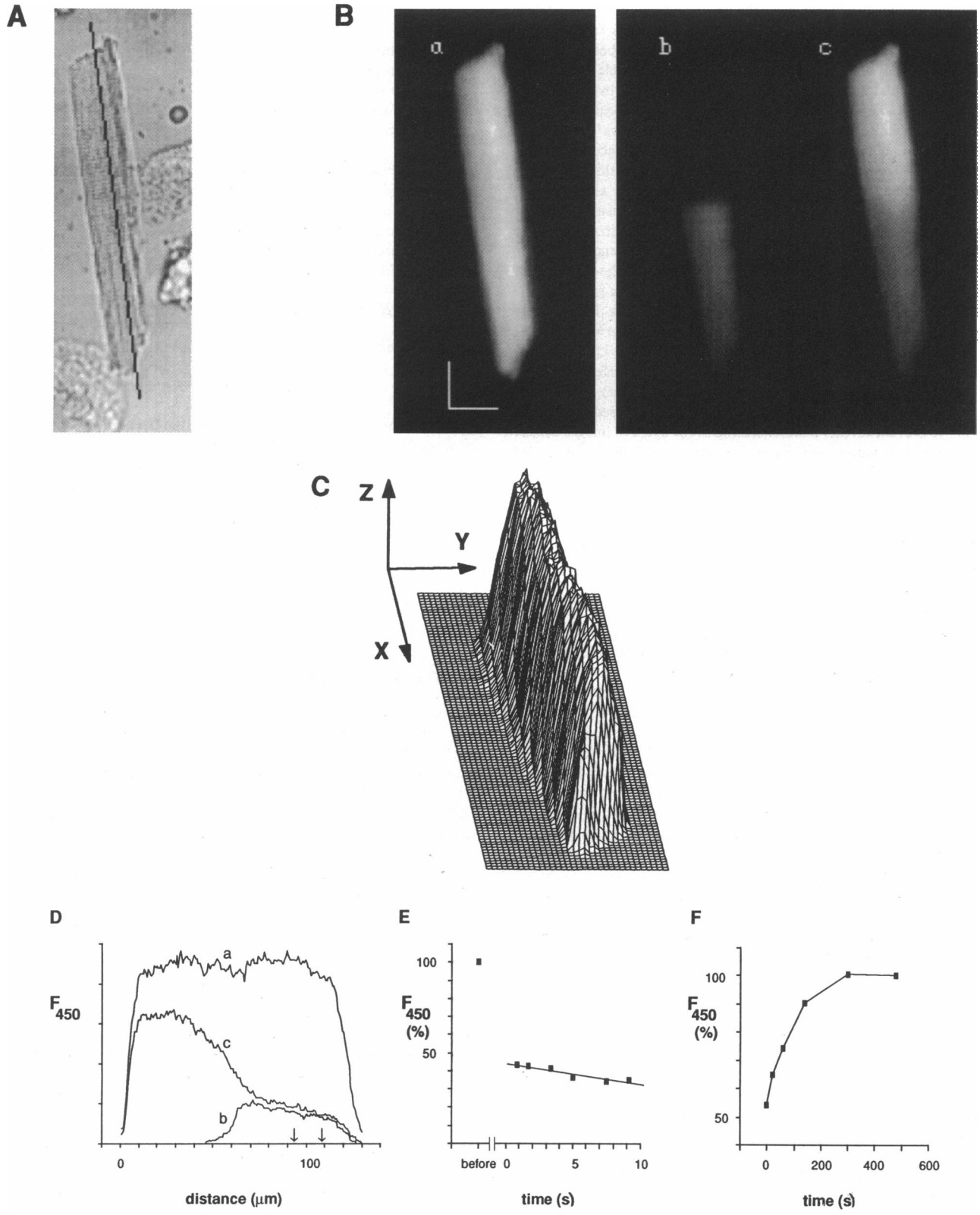
A
B
a
b
c
C
Z
Y
X
D
F_{450}
a
c
b
0
100
distance (μm)
E
100
F_{450} (%)
50
before 0
5
10
time (s)
F
100
F_{450} (%)
50
0
200
400
600
time (s)

dye, C. Fluorescence for that column was predicted by assuming that fluorescence of dye was independent of the state of the dye (free, reversibly bound or irreversibly bound) and proportional to the amount present.

Fitting the measured dye distribution with the model flourescence profile was achieved in two steps. The first step consisted in varying the fraction of dye (C''/C) that was considered to be irreversibly bound, or nondiffusible, to find the best fit between the measured *final* intracellular distribution of the dye after redistribution was completed (see Fig. 2, $A f$ and $B f$) and the prediction of the model. This process was independent of assumptions on k_{diff}, but required the assumptions that at the beginning of redistribution the fraction of dye that was irreversibly bound was the same in all elements, that diffusible and nondiffusible dye bleached at the same rate, and that there was no redistribution of dye during the period of bleaching. After this fraction (of nondiffusible dye) had been established, k_{diff} was varied, in the second step, to find the best fit to the measured data during the period of redistribution. The best fitting k_{diff} (and fraction C''/C, above) was the one for which the sum of the squares of the deviation of the observed $C_{x,t}$ from the predicted $C_{x,t}$ was the least. k_{diff} was varied in increments of 0.1 s^{-1}. Because the length of the element, x, was on average 4.27 $\times$ 10^{-4} cm, these increments in k_{diff} were equivalent to increments in D_{app} of 1.8 $\times$ 10^{-8} cm^2s^{-1}, or ~5–10% of the mean value of D_{app} estimated for fura-2 and indo-1, respectively (see Results).

The number of elements in the x dimension for the analysis of a particular cell depended on the length of the cell. In all experiments the mean of five successive pixel values along the x-axis (see Fig. 1 B) determined the value of observed fluorescence for one column of elements. The maximal possible number of elements in the z dimension was set to 14. The value for the cell height along the x-axis was derived from the fluorescence profile obtained before bleaching of the cell (see Fig. 1 D) assuming equal initial dye concentration throughout the cell and a constant fraction of nondiffusible dye in each element.

RESULTS

Photobleaching of indo-1 and fura-2

Figs. 1 and 2 illustrate the results of a representative experiment. A cardiac myocyte, previously loaded with indo-1, is shown with diascopic illumination (Fig. 1 A) and with low-intensity UV illumination (Fig. 1 B) that excites the fluorescence of indo-1.

Fig. 1 B shows the indo-1 fluorescence from the cell before masking (Fig. 1 $B a$), with the mask in place after bleaching, (Fig. 1 $B b$) and immediately after removing the mask (Fig. $B c$). Fig. 1 C shows a surface plot of the fluorescence shown in Fig. 1 $B a$, in which the height of the surface is proportional to fluorescence intensity. In Fig. 1 D are shown profiles of fluorescence intensity along the line shown in Fig. 1 A but from the images in Fig. 1 $B a$–c. Before bleaching, the fluorescence intensity is relatively uniform along the length of the cell. When the mask is in place no fluorescence is recorded from the masked region. Immediately after bleaching (Figs. 1 $B c$ and $D c$), the fluorescence intensity was reduced in both the masked and not-masked regions, but much less so in the previously masked region. The amount of dye bleached was determined from the integral of the fluorescence. The integral of a fluorescence profile (with respect to distance, x) indicates the total dye along that line (x dimension). In five indo-1 experiments (five cells), 59% (± SD 5%) of the intracellular dye, as judged by the decrease in the total fluorescence was bleached during the exposure to high-intensity UV light. In six experiments with fura-2 as the intracellular fluorescent dye only 37% (± SD 5%) of the dye was bleached during the same period, indicating that indo-1 is more susceptible to photobleaching than fura-2. Therefore, it was important to determine whether or not a significant amount of bleaching also occurred as a result of the measurements of fluorescence during the recovery period, even though the exposure to UV light was brief because the UV light was off during the long intervals between the brief measurements. An example of the integral of the indo-1 fluorescence before bleaching and during the recovery period is graphed in Fig. 1 E, as a function of the cumulative time of exposure to UV light. In the indo-1 experiments a relatively small decrease in integrated fluorescence occurred, which could be fit with a straight line over the cumulative period of exposure to UV illumination (correlation coefficient $r = 0.99$ for the averaged values of five experiments). This decrease was most probably due to additional bleaching which occurred during the measurements, and/or loss of dye. In the

FIGURE 1 (A) Image of a single guinea pig ventricular cell loaded with indo-1 visualized with diascopic illumination. The line along the longitudinal axis of the cell indicates where the profiles of intracellular fluorescence presented in D and in Figs. 2 B, a–f, were taken. (B, a) Fluorescence image of the same cell as in (A) recorded at 450 nm after background subtraction, shading correction and spatial filtering (see text). The scaling represents 20 μm vertically and 20 μm horizontally. The image is an average of 16 consecutive video frames. (B, b) Image of the cell with mask in place at the end of the 1 min exposure to high-intensity UV illumination. (B, c) Image of the cell taken immediately after removal of the mask. Fluorescence intensity of the images shown in B, b and c, has been increased by a factor of 1.5 relative to that of B, a, for purposes of display. (C) Three-dimensional plot of the fluorescence emitted from the cell shown in B, a. x, y, and z are the spatial dimensions used in the mathematical model. (D) Fluorescence profiles of images shown in B before (D, a), during (D, b), and after (D, c) bleaching. No scaling was applied to the line plots. (E) Photobleaching of indo-1: the integral of a fluorescence profile along the axis shown in A before exposure to UV light and during the redistribution phase. In this experiment the exposure to unfiltered UV light for 1 min led to a decrease to 43% of the total fluorescence recorded originally from the cell. The further decrease of cellular fluorescence during the redistribution period could be adequately related with a straight line to the cumulative time of exposure to the UV light required for the measurements (correlation coefficient in this particular experiment, $r = 0.95$). (F) Time course of dye redistribution: the average fluorescence signal recorded from the region delimited by arrows in D is plotted for different intervals after photobleaching and removal of the mask. In this experiment 95% of the final distribution was reached after 255 s.

experiments with fura-2 the change in the integrated fluorescence between beginning and termination of the dye redistribution was only ~2%. Because the change of fluorescence during the redistribution period could be fit adequately with a straight line with UV exposure time, fluorescence at any time could be readily normalized to that had been present immediately after the bleaching period. This simplified the analysis because the amount of unbleached dye in the cell could then be considered constant throughout the recovery period.

The concentrations of indo-1 and fura-2 recovered to a steady value in the bleached region. Fig. 1 *F* shows the time course of the indo-1 redistribution in the region of the bleached half-cell delimited by arrows in Fig. 1 *D*. The average pixel value of within the area delimited by arrows in Fig. 1 *D* is plotted against time, starting immediately after removal of the mask. In the five experiments with indo-1, 95% of the final dye distribution (t_{95}) was reached after 261 s (± SD 39 s). Thus, the analysis was confined to periods <600 s, because this was always sufficient time for a steady level of indo-1 to be reached. Analogous experiments with fura-2 (six cells) revealed, that the final distribution of fura-2 was reached faster: t_{95} was on average 122 s (± SD 53 s).

Figs. 2 *A*, *a–f*, illustrate the redistribution of the intracellular dye (indo-1): the image in Fig. 2 *A a* was recorded immediately after removal of the mask; images 2 *A b* to 2 *A e* were taken at various intervals after removal of the mask and show different stages of dye redistribution until the final distribution was reached (2 *A f*).

Determination of D_{app} for indo-1 and fura-2

Figs. 2 *B*, *a–f*, show line profiles of indo-1 fluorescence intensity along the line shown in Fig. 1 *A*. The noisy lines represent the actual measured fluorescence intensity (from single pixels along the longitudinal cell axis). The solid lines illustrate the prediction of Eq. 3 for a diffusion coefficient that gives the best fit to the measured data. The dashed lines indicate the prediction of Eq. 3 with a diffusion coefficient $D = 1 \times 10^{-6}$ cm^{2}s^{-1}, which would be typical for free diffusion of a molecule of the size of indo-1 and fura-2 in myoplasm (see e.g., Kushmerick and Podolsky, 1969; and Discussion). The average diffusion coefficient (D_{app}) for indo-1 in cardiac myocytes estimated by our model is 1.57×10^{-7} cm^{2}s^{-1} ± SD 0.48×10^{-7} cm^{2}s^{-1} ($n = 5$ cells). This value is approximately six times lower than that expected for free diffusion in the cytoplasm (see Discussion). D_{app} estimated for fura-2 is 3.19×10^{-7} cm^{2}s^{-1} ± SD 1.85×10^{-7} cm^{2}s^{-1} ($n = 6$ cells), a value about three times lower than expected for free myoplasmic diffusion.

Determination of the fraction of dye that does not diffuse

As discussed above, our method allowed an estimation of the fraction of intracellular dye that does not diffuse, either because it is irreversibly bound or because it is compartmentalized in organelles. Under standard loading conditions (see Methods) we estimated that on average 29% of fura-2 did not undergo diffusion, whereas in the indo-1 experiments this fraction was on average 35%.

DISCUSSION

Apparent diffusion coefficient for indo-1 and fura-2 in the cytoplasm of cardiac myocytes.

The diffusion coefficient expected for a molecule the size of indo-1 (mol wt 643) and fura-2 (mol wt 636.5) diffusing freely in the myoplasm can be obtained by interpolation of the known relationship between diffusion coefficient in myoplasm and molecular weight as reported for sorbitol, sucrose, and ATP (Kushmerick and Podolsky, 1969) and for various Ca^{2+} indicators (Maylie et al., 1987*a–c*; Hirota et al., 1989). This is summarized in Fig. 3, where the diffusion coefficients for free diffusion in myoplasm (solid symbols) as well as the apparent diffusion coefficients (open symbols) are plotted as a function of the logarithm of the molecular weight. The diffusion coefficient expected for free diffusion of indo-1 and fura-2 in myoplasm, (after adjusting for the difference in temperature by assuming a Q_{10} of 1.3 [Baylor et al., 1986]) was found by interpolation to be $\sim 1.0 \times 10^{-6}$ cm^{2}s^{-1}. The diffusion coefficient we measured for indo-1 (D_{app}), 0.157×10^{-6} cm^{2}s^{-1}, and for fura-2, 0.319×10^{-6} cm^{2}s^{-1} are also shown. Thus, our measurements indicate that the apparent diffusion coefficients for indo-1 and fura-2 in the myoplasm are only ~15–20% and 30–35%, respectively, of the value expected for free diffusion inside a muscle cell. According to Eq. 2 this small value can be explained by the fact that a rather large amount of the indicator is reversibly bound to relatively immobile sites in the myoplasm. The ratio, *R*, of bound indicator to free indicator can be calculated using Eq. 2 and the average value of D_{app}. For indo-1, *R* is 5.4, indicating that only 16% of the diffusible indo-1 is free in the myoplasm. For fura-2 we estimated D_{app} to be 0.319×10^{-6} cm^{2}s^{-1}. This value is in good agreement with values for D_{app} for fura-2 measured by Timmerman and Ashley (1986) in barnacle muscle fibers (0.39×10^{-6} cm^{2}s^{-1}; 20°C) and reported by Baylor and Hollingworth (1988) for frog skeletal muscle (0.36×10^{-6} cm^{2}s^{-1}; 16°C). In our experiments we calculated a ratio of bound fura-2 to free fura-2 of 2.1, and a fraction of 32% of diffusible fura-2 that is free.

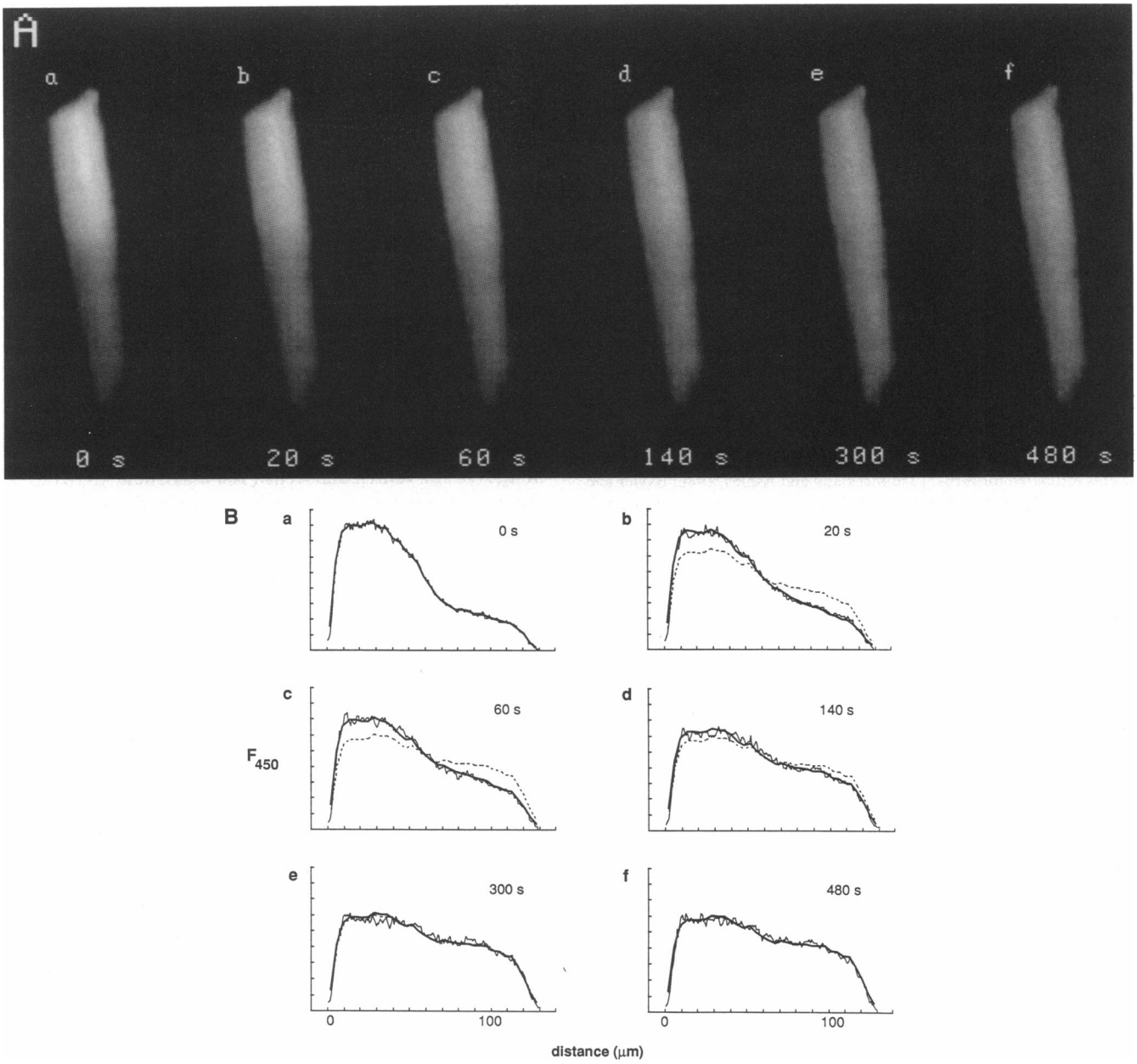

FIGURE 2 Images and fluorescence profiles of redistribution of indo-1 after photobleaching of one half of the cell. (*A*) After the lower half of the cell had been exposed to high-intensity UV light and the dye present in the other half had been prevented from photobleaching by the mask, the redistribution of the dye was recorded immediately after removal of the mask (*A*, *a*, time = 0 s) and at various intervals after that until the final distribution was reached. Image *a* was recorded at $t = 0$ s, (*A*, *b–f*) at $t = 20$, 60, 140, 300, and 480 s, respectively. (*B*) *a–f* (corresponding to images *a–f* in *A*) are experimentally recorded profiles of intracellular fluorescence along the line shown in Fig. 1 *A* and the predictions of intracellular dye diffusion by the mathematical model. The noisy line represents the measured intracellular fluorescence. The solid line is the prediction for intracellular dye diffusion using a diffusion coefficient and a fraction of nondiffusible dye that give the best fit to the data. The dashed lines represent predictions by the model using the same fraction of nondiffusible dye and a diffusion coefficient for free diffusion of a molecule of the size of indo-1 in the myoplasm.

Similar conclusions have been reached by Baylor and Hollingworth (1988) who determined a value for D_{app} for fura-2 in frog skeletal muscle approximately threefold smaller than expected for free diffusion in myoplasm. The authors point out that such a small value for D can be explained by binding of 60–65% of the intracellular dye to myoplasmic constituents. They also point out that intracellular binding of fura-2 alters the rate constants of the

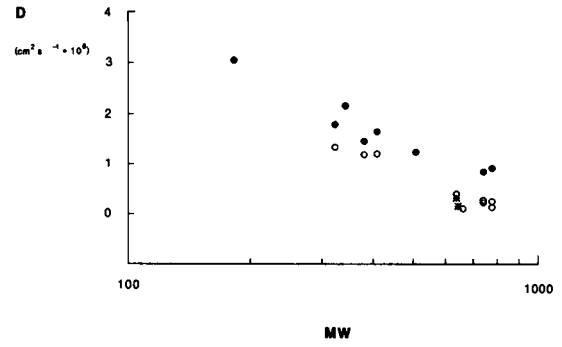

FIGURE 3 Diffusion coefficient in the myoplasm as a function of the logarithm of the molecular weight. The solid symbols represent estimates for free diffusion in the myoplasm of sorbitol, sucrose, ATP (Kushmerick and Podolsky, 1969), arsenazo III, antipyrylazo III, and tetramethylmurexide (Maylie et al., 1987*a–c*), PDAA and DMPDAA (Hirota et al., 1989). The open symbols are apparent diffusion coefficients estimated for fura-2 (Timmermann and Ashley, 1986; Baylor and Hollingworth, 1988), antipyrylazo III, arsenazo III, azo 1, tetramethylmurexide, PDAA, and DMPDAA (Baylor et al., 1986; Maylie et al., 1987*a–c*; Hirota et al., 1989). Where not obtained at 20°C, the data were adjusted to this temperature using a Q_{10} value of 1.3 (Baylor and Hollingworth, 1988). The asterisks (*) represent the value for D_{app} for indo-1 and fura-2 reported in the present study.

Ca^{2+}-fura-2 reaction in the myoplasm, and, therefore, the kinetic as well as other (spectral) properties of the indicator (Konishi et al., 1988). Intracellular binding and/or sequestration of large fractions of indicator have been reported for other intracellular Ca^{2+} indicators. Maylie et al. (1987*a* and *b*) estimated bound fractions of 73 and 68% in frog skeletal muscle for the metallochromic indicators arsenazo III and antipyrylazo III, respectively. Baylor et al. (1986) estimated that as much as 75–89% of the dyes arsenazo III, antipyrylazo III, and azo 1 are bound in the myoplasm of frog skeletal muscle cells. Intracellular binding and sequestration to a lesser extent is also reported in frog skeletal muscle for the Ca indicator tetramethylmurexide (27%; Maylie et al., 1987*c*), purpurate-3,3'diacetic acid (PDAA) and 1,1'-dimethylpurpurate-3,3'diacetic acid (DMPDAA) (19% and 27%, respectively; Hirota et al., 1989).

Intracellular compartmentalization of indo-1 and fura-2

We estimate that, on average 35% of the indo-1 and 29% of fura-2 inside cardiac myocytes is not diffusible, when the myocytes are loaded as we did with the membrane permeant ester form (/AM) of these fluorescent indicators. This could result either from irreversible binding or from "trapping" or compartmentalization of the dyes in organelles. It is known that incompletely hydrolyzed indicator molecules can become associated with intracellular organelles. For example, polymorphonuclear leukocytes exposed to fura-2/AM develop a trapped, Ca^{2+}-insensitive, highly-fluorescent species, that is probably incompletely deesterified fura-2/AM (Scanlon et al., 1987). Almers and Neher (1985) provide evidence that ester-loaded fura-2 accumulates to a significant degree in the secretory granules of mast cells. In rabbit hearts (Lee et al., 1988) that were exposed to indo-1/AM, 72% of the dye was in the cytosol, and the remainder was associated with the mitochondria, microsomes and the nucleus. Isolated liver mitochondria have been shown (Gunter et al., 1988) to be able to take up fura-2/AM and to hydrolyze it fully inside the organelle. Because mitochondria occupy 35–40% of the cardiac cell volume (Sommer and Jennings, 1986), this is expected to be a particularly important problem in cardiac cells. In fact, heterogeneities of fura-2 fluorescence have been interpreted in images of rat ventricular cells (Jou and Sheu, 1990) to be due to indicator trapped in mitochondria. Spurgeon et al. (1990) estimate that as much as 51% of indo-1 present in rat ventricular cells loaded with indo-1/AM is found in the mitochondria.

Use of fura-2/AM and indo-1/AM in physiological experiments

Compartmentalization of dye in organelles introduces severe problems in the estimation of cytoplasmic $[Ca^{2+}]$, the quantity that is usually desired in physiological experiments. Digital imaging fluorescence microscopy has the potential to resolve these problems, by providing a way to observe separately the fluorescence that arises from cytoplasm and that from organelles. The spatial resolution of the imaging techniques available currently must be improved substantially, however, before this could actually be done. In cells that can be subjected to whole-cell voltage clamp, the solution to the problem would seem to be to introduce the membrane-impermeant forms of the indicators via diffusion from the micropipette electrode, as is routinely done in experiments on mammalian cardiac cells (e.g., Beuckelmann and Wier, 1988). We note though that lack of compartmentalization in that case has not been verified experimentally. We did not do so in the present experiments because the micropipette electrode provides an additional, time-varying (as access resistance changes) source of unbleached indicator that would be difficult to account adequately.

In frog skeletal muscle, reversible binding of fura-2 to cytoplasmic constituents may alter the kinetics of the reaction of fura-2 with Ca^{2+} (Baylor and Hollingworth, 1988; Klein et al., 1988). The extent to which kinetics of fura-2 may have been altered in the guinea-pig cardiac cells we studied is unknown. Sipido and Wier (1991) have examined the effects of different assumptions about

kinetic rate constants on the calculation of $[Ca^{2+}]_i$ transients from fura-2 signals in guinea-pig ventricular cells. If the "on" rate constant is assumed to be at the lower limit of that estimated in skeletal muscle (1.0×10^7 $M^{-1}s^{-1}$) and the "off" rate constant is assumed to be 23 s^{-1} (Baylor and Hollingworth, 1988), then resting $[Ca^{2+}]_i$ is calculated to be $\sim 1 \times 10^{-6}$ M, a value that is implausibly high. Nevertheless, the possibility that rate constants are altered to this extent also in cardiac muscle cannot be excluded unequivocally until kinetic data can be obtained from cells loaded with fura-2.

Financial Support was provided by The Graduate School, University of Maryland at Baltimore, through Designated Research Initiative Funds, by the Medical Biotechnology Center, and by the United States Public Health Service (HL 29473).

Received for publication 21 May 1990 and in final form 27 July 1990.

REFERENCES

Almers, W., and E. Nehers. 1985. The Ca signal from fura-2 loaded mast cells depends strongly on the method of dye-loading. *FEBS (Fed. Eur. Biochem. Soc.) Lett.* 192:13–18.

Barcenas-Ruiz, L., and W. G. Wier. 1987. Voltage dependence of intracellular $[Ca^{2+}]_i$ transients in guinea pig ventricular myocytes. *Circ. Res.* 61:148–154.

Baylor, S. M., and S. Hollingworth. 1988. Fura-2 calcium transients in frog skeletal muscle fibres. *J. Physiol. (Lond.).* 403:151–192.

Baylor, S. M., W. K. Chandler, and M. W. Marshall. 1982. Dichroic components of arsenazo III and dichlorophosphonazo III signals in skeletal muscle fibres. *J. Physiol. (Lond.).* 331:179–210.

Baylor, S. M., S. Hollingworth, C. S. Hui, and M. E. Quinta-Ferreira. 1986. Properties of the metallochromic dyes arsenazo III, antipyrylazo III and azo 1 in frog skeletal muscle fibres at rest. *J. Physiol. (Lond.).* 377:89–141.

Beuckelmann, D. J., and W. G. Wier. 1988. Mechanism of release of calcium from sarcoplasmic reticulum of guinea-pig cardiac cells. *J. Physiol. (Lond.).* 405:233–255.

Crank, J. 1975. The Mathematics of Diffusion. Oxford University Press, Ely House, London. 2–4, 326–327.

Grynkiewicz, G., M. Poenie, and R. Tsien. 1985. A new generation of Ca^{2+} indicators with greatly improved fluorescence properties. *J. Biol. Chem.* 260:3440–3450.

Gunter, T. E., D. Restrepo, and K. K. Gunter. 1988. Conversion of esterified fura-2 and indo-1 to Ca^{2+}-sensitive forms by mitochondria. *Am. J. Physiol.* 255:C304–C310.

Hirota, A., W. K. Chandler, P. L. Southwick, and A. S. Waggoner. 1989. Calcium transients recorded from two new purpurate indicators inside frog cut twitch fibers. *J. Gen. Physiol.* 94:597–631.

Jou, M.-J., and S. S. Sheu. 1990. Spatial distribution of intracellular Ca^{2+} and the possible role of organelle buffering in cultured neonatal rat ventricular myocytes. *Biophys. J.* 57:343a. (Abstr.)

Kao, J. P. Y., and R. Y. Tsien. 1988. Ca^{2+} binding kinetics of fura-2 and azo-1 from temperature-jump relaxation measurements. *Biophys. J.* 53:635–639.

Klein, M. G., B. J. Simon, G. Szucs, and M. F. Schneider. 1988. Simultaneous recording of calcium transients in skeletal muscle using high- and low-affinity calcium indicators. *Biophys. J.* 53:971–988.

Konishi, M., A. Olson, S. Hollingworth, and S. M. Baylor. 1988. Myoplasmic binding of fura-2 investigated by steady-state fluorescence and absorbance measurements. *Biophys. J.* 54:1089–1104.

Kushmerick, M. J., and R. J. Podolsky. 1969. Ionic mobility in muscle cells. *Science (Wash. DC).* 166:1297–1298.

Lee, H., R. Mohabir, N. Smith, M. R. Franz, and W. T. Clusin. 1988. Effect of ischemia on calcium-dependent fluorescence transients in rabbit hearts containing indo-1. Correlation with monophasic action potentials and contraction. *Circulation.* 78:1047–1059.

Maylie, J., M. Irving, N. L. Sizto, and W. K. Chandler. 1987*a*. Comparison of arsenazo III optical signals in intact and cut frog twitch fibers. *J. Gen. Physiol.* 89:41–81.

Maylie, J., M. Irving, N. L. Sizto, and W. K. Chandler. 1987*b*. Calcium signals recorded from cut frog twitch fibers containing antipyrylazo III. *J. Gen. Physiol.* 89:83–143.

Maylie, J., M. Irving, N. L. Sizto, G. Boyarsky, and W. K. Chandler. 1987*c*. Calcium signals recorded from cut frog twitch fibers containing tetramethylmurexide. *J. Gen. Physiol.* 89:41–81.

Scanlon, M., D. A. Williams, and F. S. Fay. 1987. A Ca^{2+}-insensitive form of fura-2 associated with polymorphonuclear leukocytes. *J. Biol. Chem.* 262:6308–6312.

Sipido, K. R., and W. G. Wier. 1991. Flux of Ca^{2+} across the sarcoplasmic reticulum of guinea-pig cardiac cells during excitation-contraction coupling. *J. Physiol. (Lond.).* In press.

Sommer, J. R., and R. B. Jennings. 1986. Ultrastructure of cardiac muscle. *In* The Heart and Cardiovascular System. H. A. Fozzard et al., editors. Raven Press Ltd. New York. 61–100.

Spurgeon, H. A., M. D. Stern, G. Baartz, S. Raffaeli, R. G. Hansford, A. Talo, E. G. Lakatta, and M. C. Capogrossi. 1990. Simultaneous measurement of Ca^{2+}, contraction and potential in cardiac myocytes. *Am. J. Physiol.* 258:H574–H586.

Takamatsu, T., and W. G. Wier. 1990*a*. Calcium waves in mammalian heart: quantification of origin, magnitude, waveform, and velocity. *FASEB (Fed. Am. Soc. Exp. Biol.) J.* 4:1519–1525.

Takamatsu, T., and W. G. Wier. 1990*b*. High-temporal resolution video imaging of intracellular calcium. *Cell Calcium.* 11:111–120.

Timmermann, M. P., and C. C. Ashley. 1986. Fura-2 diffusion and its use as an indicator of transient free calcium changes in single striated muscle cells. *FEBS (Fed. Eur. Biochem. Soc.) Lett.* 209:1–8.

Williams, D. A., K. E. Fogarty, R. Y. Tsien, and F. S. Fay. 1985. Calcium transients in single smooth muscle cells revealed by the digital imaging microscope using Fura-2. *Nature (Lond.).* 318:558–561.